

# Development of piezoresistive PDMS/MWCNT foam nanocomposite sensor with ultrahigh flexibility and compressibility

Journal of Intelligent Material Systems and Structures

2022, Vol. 33(14) 1751–1761

© The Author(s) 2021



Article reuse guidelines:

sagepub.com/journals-permissions

DOI: 10.1177/1045389X211064345

journals.sagepub.com/home/jim



Pardis Ghahramani, Kamran Behdinan and Hani E. Naguib

## Abstract

Polymer foam nanocomposites attract great interest in many wide ranges of biomedical and healthcare monitoring applications. In this study, we investigated the effect of porosity and multi-walled carbon nanotube (MWCNT) content on the piezoresistivity, sensitivity, and mechanical properties of Polydimethylsiloxane (PDMS)/MWCNT foam nanocomposite. The foam nanocomposites were fabricated by particulate leaching method and their electrical and mechanical characteristics were investigated using the different porosity levels (60% and 70%) and different conductive nanofiller contents (0.5 wt.% and 1 wt.%). The foam nanocomposites with 0.5 wt.% MWCNT content and 60% porosity possessed higher pressure sensitivity, higher gage factor, and lower electrical hysteresis along with higher mechanical properties. Moreover, fabricated PDMS/MWCNT foam nanocomposite demonstrated high flexibility, high compressibility, and high recoverability in addition to limited mechanical hysteresis (less than 3%) with a large dynamic sensing range. Contrary to the existing foam nanocomposite samples in the literature, PDMS/MWCNT foam nanocomposites withstood higher pressure ranges (3.5–5 MPa) at limited thickness (average 2.3 mm) without experiencing noticeable macroscopic damage.

## Keywords

Piezoresistive, foam nanocomposite, force mapping, PDMS, MWCNT

## 1. Introduction

The applications of flexible piezoresistive sensors in biomedical science are gradually increased over the last decade (Iglío et al., 2018; Zuruzy et al., 2017). The development of novel flexible highly sensitive pressure-detecting sensors with high durability, biocompatibility, and lightweight has drawn tremendous attention toward smart systems and wearable healthcare devices (Amjadi et al., 2016; Chortos et al., 2016; Park et al., 2015).

Flexible piezoresistive foam nanocomposite sensor is a novel type of pressure-sensitive sensors which operates based on resistivity change in the material while an external force is applied to it (Li et al., 2014; Liu et al., 2016; Zhou et al., 2016). This sensor has peculiar features which makes it a sound choice to be used for pressure-detecting in biomedical and health monitoring applications (Tung et al., 2016; Yamada et al., 2011; Zhao et al., 2010). These features include high flexibility, high sensitivity, lightweight, high mechanical resistance for damage protection, and easy manufacturing

process (Xu et al., 2018). Due to the high flexibility and high sensibility of foam nanocomposite sensor, it has a potential application in the artificial knee joint for force mapping in our future work. Embedment of the piezoresistive sensor between the Femoral and Tibial components of an implant can facilitate the process of detecting artificial knee plantar pressure map. As a result, the applied pressure distribution on the artificial knee can be obtained (Bar-Ziv et al., 2010; Schurman

Department of Mechanical and Industrial Engineering, University of Toronto, Toronto, ON, Canada

### Corresponding authors:

Kamran Behdinan, Department of Mechanical and Industrial Engineering, University of Toronto, 5 King's College Road, Toronto, ON M5S 3G8, Canada.

Email: behdinan@mie.utoronto.ca

Hani E. Naguib, Department of Mechanical and Industrial Engineering, University of Toronto, 5 King's College Road, Toronto, ON M5S 3G8, Canada.

Email: naguib@mie.utoronto.ca

and Smith, 2004). The recorded results from the pressure sensor can be used to detect the accuracy and further adjustment of the designed biomechanical system (Tanabe et al., 2017).

It is believed that the electron conduction in the nanocomposites consists of three main mechanisms: the intrinsic conductance of the conductor fillers, the direct contact conductance, and the conductance resulting from electron tunneling between conducting fillers. The tunneling resistance in the nanocomposites is influenced by several parameters including polymer dielectric properties, the tunneling gap between adjacent conductive fillers, and the electronic structure of the nanotubes (Bao et al., 2012; Kanoun et al., 2021; Zare and Rhee, 2021).

The critical conductive filler content, also known as the electrical percolation threshold, provides conductivity for the nanocomposite (Bauhofer and Kovacs, 2009; Bloor et al., 2005; Ding et al., 2017). In nanocomposites, if the conductive particles are isolated from each other by an insulating matrix and the gap between them is less than the critical distance, the interparticle tunneling will help to improve the conductivity of nanocomposite (Oskouyi et al., 2014). Moreover, reducing the gaps between the neighbor particles (fillers) and using particles with a higher aspect ratio (length to diameter ratio) increase the particle interconnectivity which improves the conductivity inside the nanocomposites (Choi et al., 2019). Zheng et al. (2004) and Ameli et al. (2014) showed that conductive foam nanocomposites have lower percolation thresholds in comparison to corresponding nonporous nanocomposites. Due to the volume exclusion in foam nanocomposite structure, the available polymer matrix for the dispersion and distribution of the particles is reduced and higher particles interconnectivity is achievable (Ameli et al., 2014). Figure 1 is the schematic illustration of volume exclusion microstructural effect on improving particles interconnection in the foam structure.

Ameli et al. (2014) investigated the effect of relative density and cellular structure of micro/nanocellular PP/MWCNT nanocomposite on the electrical

conductivity. They revealed that by increasing volume expansion through foaming, the electrical percolation threshold decreases more than fivefold, from 0.50 down to 0.09 vol.%. However, the effect of foaming on the piezoresistive behavior of foam nanocomposite is not investigated in this study. Madaleno et al. (2013) showed that the compressive properties of PU/CNT foam nanocomposites are enhanced in comparison to pure PU foam. Iglio et al. (2018) prepared piezoresistive PDMS foam sensors decorated with pristine MWCNTs by drop-casting of CNT ink drops. The fabricated sensors demonstrated reliable detection in health monitoring applications within a working range up to 50 kPa at the optimum CNT density of 25 mg/cm<sup>3</sup>. Although Iglio et al. worked on the specific foam porosity and cell size, the study of foam morphology and porosity effects on the piezoresistivity are missing in their study.

Many successful foam nanocomposites with great advantages in pressure sensing are reported in the literature; however, most of them suffer from poor mechanical properties and inferior recoverability (Huang et al., 2017). Studies show that in normal walking,  $2.5\text{--}2.8 \times$  bodyweight force will be applied to the knee joint (D'Lima et al., 2012). The pressure sensor which is going to be embedded in the artificial knee joints should be compatible with the amount of pressure that applies to the joints. However, one of the drawbacks of fabricated sensors in the literature is the limited force working range (Iglio et al., 2018). To the best of our knowledge, the existing foam pressure sensors are able to be used for up to 900 kPa which shows that majority of the studies on foam nanocomposite sensors focus on low-pressure applications (Kim and Kim, 2017). Moreover, most porous nanocomposites suffer from low Young's modulus and weak compressive strength which limit their applications (Cai et al., 2020; Cao et al., 2019; Chen et al., 2018; Tang et al., 2019). Insensitive behavior at larger strain levels (more than 30%), due to the saturation of conductive networks at low strains (less than 10%), is another weakness that is reported in the foam nanocomposites (Patole et al.,

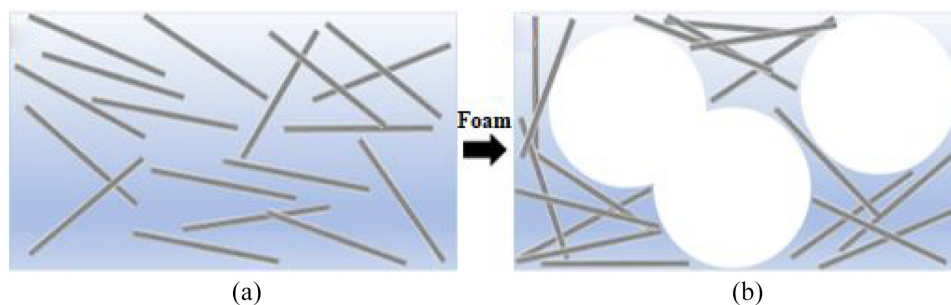


**Figure 1.** Schematic illustration of the volume exclusion microstructural effect on improving particles interconnection: (a) solid nanocomposite and (b) foam nanocomposite.

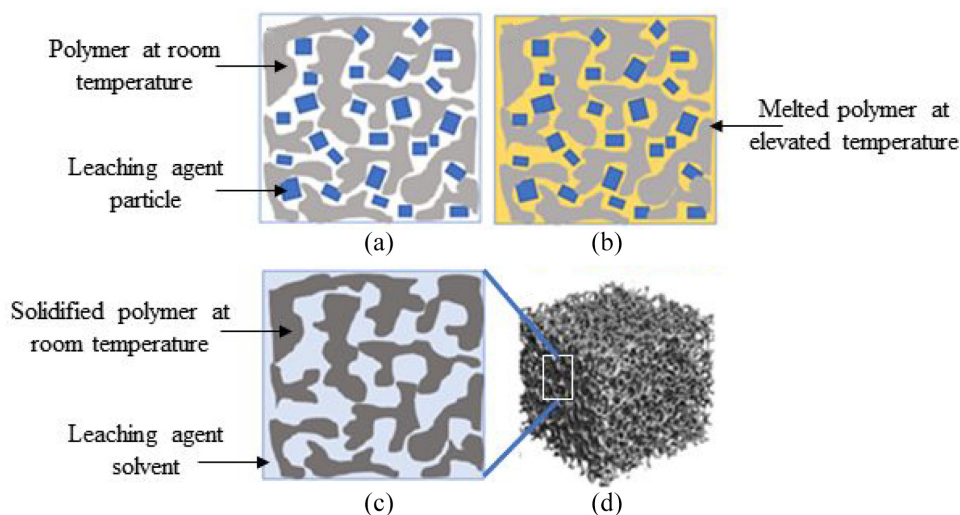


**Figure 2.** Schematic of particulate leaching process: (a) polymer and leaching agent mixing, (b) heating the mixture to melt the polymer, (c) leaching agent extraction by solvent, and (d) porous structure.

2019). Furthermore, most of the current foam nanocomposites have high thicknesses (more than 6 mm) which hinder their applications for cases that require thinner sensors (Boland et al., 2018; Liu et al., 2017; Rinaldi et al., 2016).

Therefore, the deliverable of this paper is to tailor the ultra-flexible PDMS/CNT piezoresistive foam nanocomposite structure with elevated Young's modulus, mechanical strength, compressibility, and recoverability in addition to limited hysteresis effect. Moreover, another key target in this study is to achieve a higher pressure-sensor detecting range at a low thickness which can broaden the applications of PDMS/CNT foam nanocomposite in force mapping. In this research, open-cell foam PDMS/MWCNT nanocomposites with 60% and 70% leaching agent contents and 0.5 wt.% and 1 wt.% MWCNT contents were fabricated by a combination of mold casting-particulate leaching methods. The advantage of this foaming technique is obtaining higher controllability over the pore sizes and density in the foam structure (Rinaldi et al., 2016). The particulate leaching method is more environmentally friendly than the chemical foaming process and has an easy and cost-effective manufacturing process (Ma et al., 2021). PDMS has excellent advantages including commercial availability, excellent flexibility, well-researched properties, chemical inertness, stability over a wide range of temperatures, variable mechanical properties, and biocompatibility which made it the right choice for this research (Hammock et al., 2013).

MWCNT was chosen as the conductive reinforcement candidate for the fabrication of foam nanocomposite due to its significant advantages such as excellent electrical conductivity, outstanding mechanical properties, and high aspect ratio (Choi et al., 2019). In this article, the effect of filler contents, foam morphology,

and porosity on the piezoresistivity, pressure sensitivity, and mechanical properties (cyclic and monotonic) of the PDMS/MWCNT foam nanocomposite were investigated.

## 2. Experimentation

### 2.1. Preparation of open-cell PDMS/MWCNT foam nanocomposite

In this study, PDMS/MWCNT nanocomposite mixture was foamed by the particulate leaching foaming method and Figure 2 shows the schematic of the particulate leaching process (Ødegaard et al., 2000).

Samples with 60 wt.% and 70 wt.% leaching agent contents were prepared at 0.5 wt.% and 1 wt.% MWCNT contents to fabricate PDMS/MWCNT foam nanocomposite. Since the literature reported 1 wt.% MWCNT is close to the percolation threshold of PDMS foam nanocomposites (Ameli et al., 2014; Madaleno et al., 2013; Ramalingame et al., 2017), the effect of 1 wt.% and 0.5 wt.% filler contents on the piezoresistivity of PDMS/MWCNT foam nanocomposite were investigated. In this study, 60 wt.% and 70 wt.% leaching agent contents were used in the foam fabrication process to achieve the best result. Less than 60% leaching agent content can adversely affect the complete citric acid leaching process in foam structure, and more than 70% leaching agent content can lead to a fragile foam structure with reduced mechanical strength (Ghahramani et al., 2021). The samples are entitled as 70%–0.5% (foam nanocomposites with 70 wt.% leaching agent content and 0.5 wt.% MWCNT content), 70%–1% (foam nanocomposites with 70 wt.% leaching agent content and 1 wt.% MWCNT content), and 60%–0.5% (foam

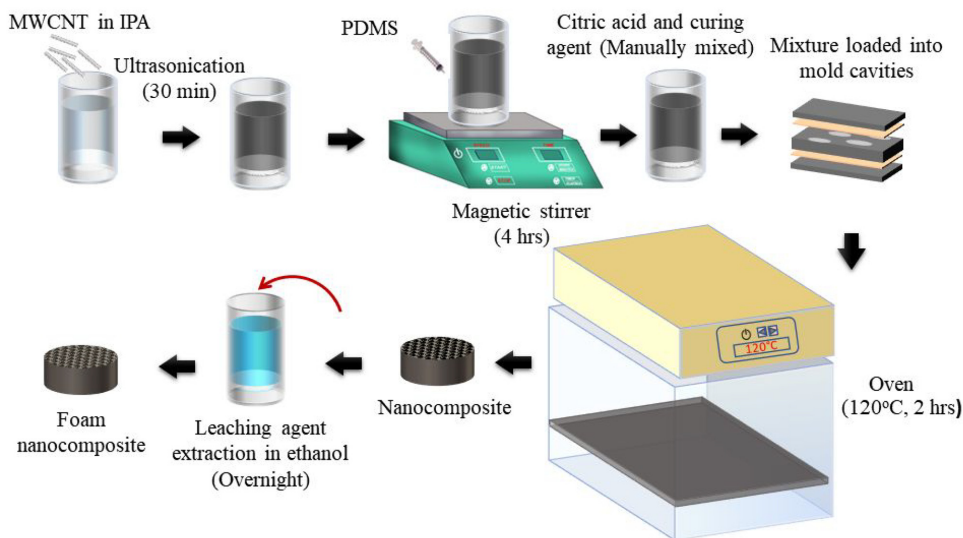


**Figure 3.** Schematic of the preparation process of PDMS/MWCNT foam nanocomposites.

nanocomposites with 60 wt.% leaching agent content and 0.5 wt.% MWCNT content). Figure 3 shows a schematic of PDMS/MWCNT foam nanocomposite preparation process. Based on the target volume of the mold cavities and the desired number of samples at beginning of the experiment, a specific amount of PDMS (Sylgard 184 two-component Dow Corning) was weighed. For different types of samples, 0.5 wt.% and 1 wt.% of the weighed PDMS were collected from MWCNT particles (Shengzhen Nanotech Port Co. Ltd, diameters: 9.5 nm, length: 1.5  $\mu\text{m}$ ). Besides, citric acid particles were weighed according to the collected PDMS with 6:3 and 7:3 mass ratios (citric acid to PDMS) for fabrications of samples with 60% and 70% porosity, respectively. In the fabrication process, MWCNT was dispersed in 80 ml Isopropyl alcohol (IPA) by a tip sonicator (QSonica, Q700). The sonication processing time was 30 min while the pulse mode was adjusted to 4 s on and 2 s off to reduce the heat gain in the nanocomposite. The amplitude was set at 100% and the temperature of the mixture was controlled with an ice bath. Then, PDMS was added to the solution and was mixed by a magnetic stirrer for 4 h to completely extract the IPA. The PDMS curing agent (Sylgard, 1:10 weight ratio for PDMS to curing agent) was added to the mixture to help polymer crosslinking. Then, citric acid was added and manually mixed with the solution to reach a homogeneous mixture. The final mixture was poured into the cavities (24 mm diameter, 2.3 mm thickness) of an Aluminum mold. The mold was at room temperature and then was put in an oven at 120°C for 2 h to cure the mixture. After curing, samples were removed from the mold and submerged in ethanol overnight to extract the leaching agent and then were dried in the oven at 90°C for 4 h. Since ethanol is able to wet the PDMS foam and citric acid is

highly soluble in ethanol, these materials were proper candidates to be used during the particulate leaching process (Li et al., 2017).

### 2.1.1. Characterization

The compression tests were carried out by Instron Universal testing machine (INSTRON 5944) under force control (1 mm/min) displacement mode.

The electrical resistance of foam nanocomposites was directly measured by the two-electrode method using a Keithley 2100 digital multimeter which was connected to the Instron. The experimental setup for piezoresistive response measurement is illustrated in Figure 4. In the two-electrode method, two surfaces of Instron platens were covered with insulative tape to eliminate their conductivity effect on the piezoresistive responses of the samples. Then two copper electrodes were cut according to Figure 4 and their head were taped to the center of the top and bottom platens of Instron.

The electrodes head had the same diameter as the samples (24 mm). Multimeter probes were connected to each electrode tail. Then, the sample was fixed on the bottom electrode and the top platen was manually displaced to decrease the distance between the platens. Once the top platen and sample touched each other, the multimeter showed a change in the sample electrical resistance. That is when the force and displacement of the Instron were balanced and the automatic compression test with a 1 mm/min displacement rate was started. The electrical resistance data of the sample in response to the applied force were simultaneously recorded by the multimeter.

Morphologies of the fabricated foams were characterized by using scanning electron microscopy (SEM). To prepare the foams for microscopy, their



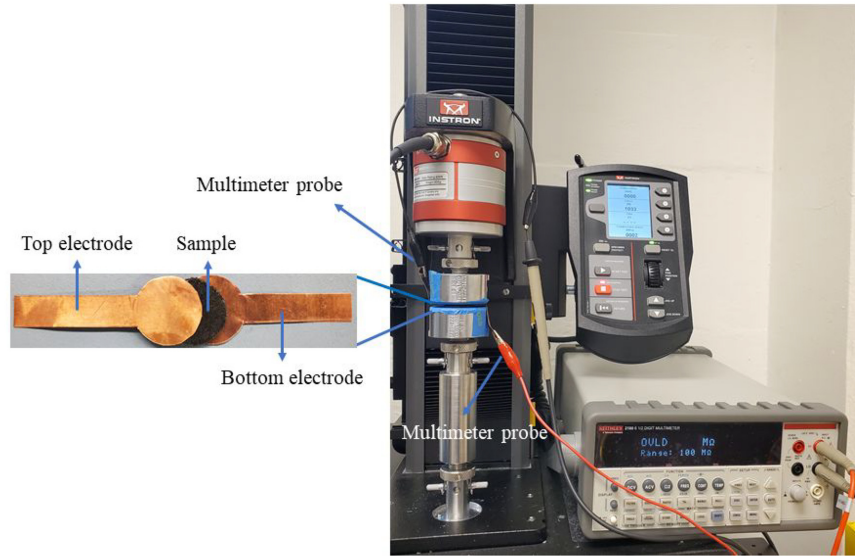


**Figure 4.** Experimental setup for piezoresistive response measurement.

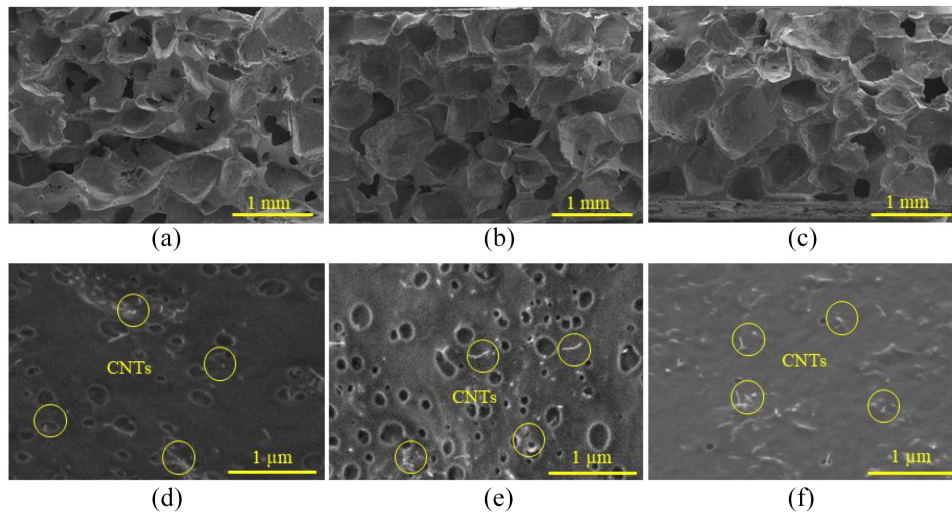


**Figure 5.** Morphology of PDMS/MWCNT foam nanocomposites: (a) 70%–0.5%, (b) 70%–1%, and (c) 60%–0.5%. MWCNT dispersion in PDMS/MWCNT foam nanocomposites: (d) 70%–0.5%, (e) 70%–1%, and (f) 60%–0.5%.

cross-sections were exposed to cryo-fracturing under liquid nitrogen and the fractured surfaces were then sputter-coated with gold. The cell diameters in the foam nanocomposite structures were determined by using ImageJ analysis software.

The sensitivity of piezoresistive materials was quantified by the gage factor (GF) value which is defined in equation (1):

$$GF = \left( \frac{\Delta R}{R_0} \right) / \varepsilon \quad (1)$$

where  $R_0$  is the initial electrical resistance of the material before applying the force,  $\Delta R$  is the material electrical resistance change in response to the compression,

and  $\varepsilon$  is the compressive strain which represents the relative displacement in sample thickness.  $\varepsilon$  is defined in equation (2):

$$\varepsilon = \frac{L_1 - L_2}{L_1} \quad (2)$$

where  $L_1$  is the initial sample thickness before applying external pressure, and  $L_2$  is the final sample thickness when the sample is under external pressure.

### 3. Results and discussion

The effects of leaching agent content on the morphology of open-cell PDMS foams were analyzed by SEM.

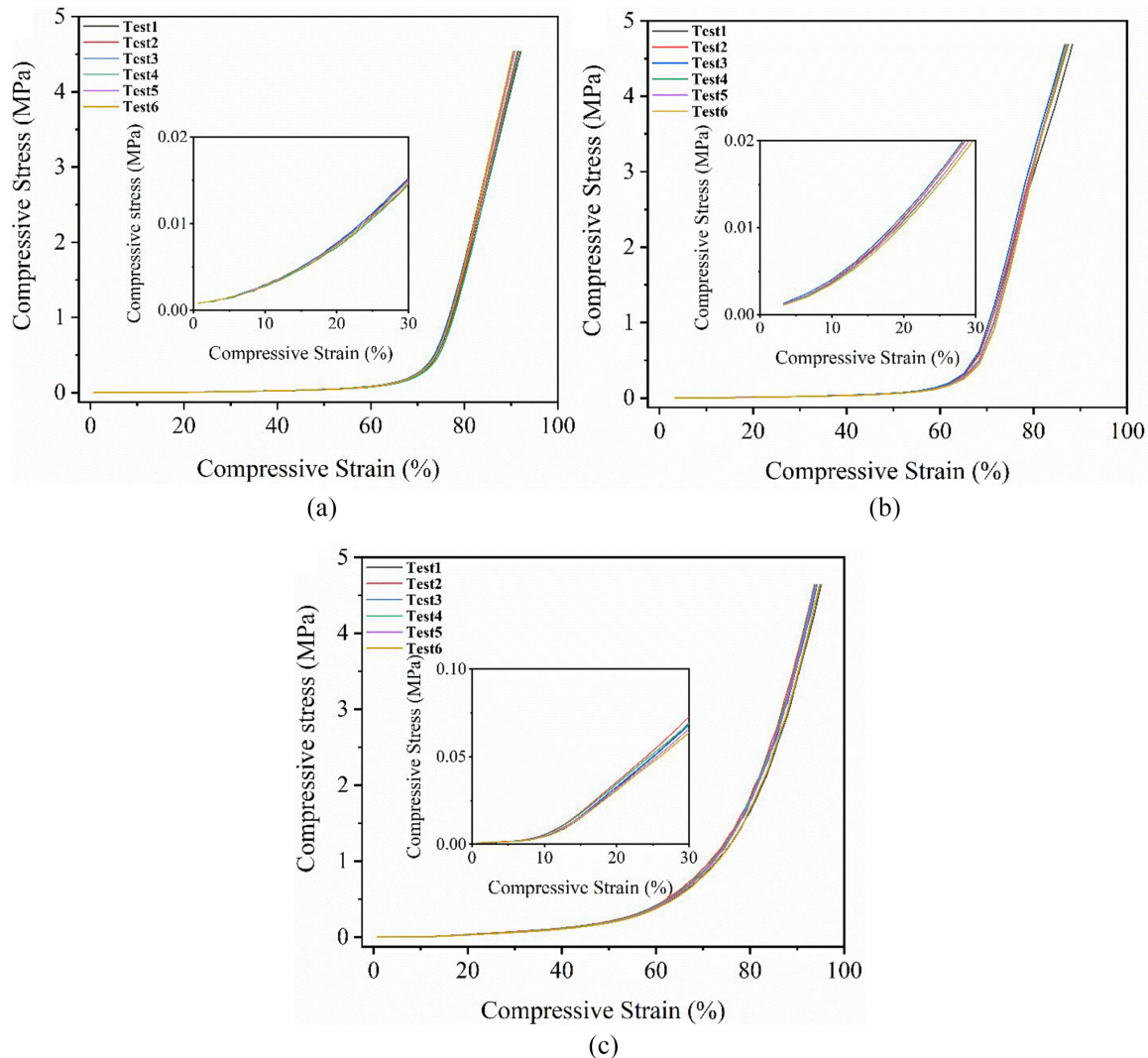


**Figure 6.** Stress versus strain in six different cycles for foam nanocomposites: (a) 70%–0.5%, (b) 70%–1%, and (c) 60%–0.5%.

Figure 5 shows SEM micrographs of three open-cell foam nanocomposites obtained at different magnifications. It can be observed that all foams have a large number of voids, which provided high foam porosity. Moreover, SEM micrographs indicate that citric acid particles were properly dispersed in the polymer matrix and huge voids, which can be the result of bulky citric acid agglomerations, were not observed inside the foam structure. The cells sizes in the SEM micrographs imply that the voids are a negative replica of citric acid particles. Besides the SEM micrographs, the weight differences of the samples before and after the particulate leaching process indicated more than 98% particle extraction which proved that the pores in the open-cell foams are highly interconnected.

Figure 5(a) to (c) illustrate that the samples with 70% leaching agent content contain more voids than the sample with 60% leaching agent. Moreover, Figure 5(d) to (f) show a good MWCNT dispersion

throughout the polymer matrix for all the samples. In these figures, some of the MWCNT particles are identified by yellow circles. The proper dispersion of MWCNTs may result in consistent piezoresistive behavior in the foam nanocomposite samples.

Figure 6 plots the stress versus strain graphs of three different types of foam nanocomposite at six cycles (runs). The cycles were consecutively performed at a 1 mm/min displacement rate with a 1 min relaxation time between each individual cycle. A maximum of 2 kN force was applied to the samples in each cycle.

These graphs indicate that foam nanocomposites had very similar behavior through different cycles of mechanical testing. The high repeatability of mechanical properties of foam nanocomposites, which originates from their limited hysteresis effect (less than 3%), makes them a reliable choice for controllable sensing applications. High flexibility, uniform foam morphology, stable pores, and strong cell walls in the foam

**Table 1.** Young's modulus of three different PDMS/MWCNT foam nanocomposites.

Samples name	Average Young's modulus (kPa)	Standard deviation (kPa)	$R^2$
60%–0.5%	233	15.3	0.9571
70%–0.5%	47	5.7	0.9417
70%–1%	88	5	0.9810

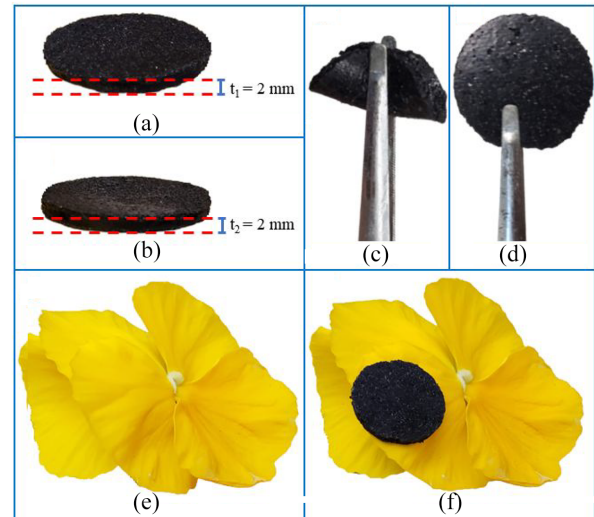
structure resulted in a very low mechanical hysteresis in the PDMS/MWCNT foam nanocomposites which is a huge advantage over the reported foam nanocomposites in the literature (Cai et al., 2020; D'Lima et al., 2012; Hammock et al., 2013; Rinaldi et al., 2016).

According to Figure 6, foam nanocomposites with 70% porosity experienced larger displacement at the same external stress comparing to the sample with 60% porosity in the elastic region. Normally, foam samples with higher porosity are expected to undergo a larger strain at a given pressure (Kim et al., 2019). Moreover, the presence of MWCNT in the foam matrix increases the mechanical strength of foam samples to a large extent. Therefore, Figure 6 indicates that 70%–1% sample (which had higher MWCNT content) has a lower strain at the same compressive stress comparing to the 70%–0.5% sample.

The average Young's modulus of three different types of PDMS/MWCNT foam nanocomposites is shown in Table 1. Young's modulus of each foam nanocomposite was determined from the trendline slope of the linear elastic region of the compressive stress-compressive strain curve from 0% to 30% compressive strain. Moreover, Table 1 presents the average  $R^2$  value for the linear trendline of compressive stress-compressive strain graphs from 0% to 30% compressive strain.  $R^2$  values indicate that the initial slopes (up to 30% compressive strain) of compressive stress-compressive strain curves are acceptably linear.

The results indicate that 60%–0.5% samples, due to the lower porosity, had a much higher Young's modulus in comparison to 70%–0.5% or 70%–1% samples. Moreover, 70%–1% samples had higher Young's modulus than 70%–0.5% samples because of higher MWCNT content. In this research, PDMS/MWCNT foam nanocomposites had higher Young's modulus in comparison to similar studies, and the reasons can be listed as the uniform and stable foam morphology, sufficient MWCNT dispersion in the polymer matrix, and strong cell walls without experiencing collapse or macroscopic deformation under elevated stresses (up to 4 MPa) (Chen et al., 2018; Huang et al., 2017; Tang et al., 2019).

Compression tests were conducted for six cycles and each time the thickness of the samples was measured

**Figure 7.** Flexibility and lightweight of PDMS/MWCNT foam nanocomposite: (a) before compression test, (b) after compression test, (c) bending the sample with a tweezer, (d) sample after bending with no sign of fracture, and (e and f) the lightweight sample standing on top of a flower.**Table 2.** Weight and density of PDMS/MWCNT foam nanocomposites.

Samples name	Average weight (g)	Average density ( $\text{g/cm}^3$ )
60%–0.5%	0.53	0.51
70%–0.5%	0.45	0.39
70%–1%	0.46	0.40

immediately after the testing. The results showed that PDMS/MWCNT foam nanocomposites could be compressed more than 85% and their thickness was returned to the primary thickness which reveals their high flexibility, compressibility, and recoverability (Cai et al., 2020). Figure 7(a) and (b) present the PDMS/MWCNT foam nanocomposite physical shape before and after the compression test, respectively. According to Figure 7(c), foam nanocomposite could be bent more than almost  $180^\circ$  and then return to its original shape (Figure 7(d)) without any fracture which confirms its excellent flexibility. Having a lightweight is another great feature of PDMS/MWCNT foam nanocomposite which is demonstrated in Figure 7(e) and (f). In Figure 7(f), the porous nanocomposite is placed on top of a petal without bending it which proves the lightweight of the sample. In addition, PDMS/MWCNT foam nanocomposites have significantly low density (as low as  $0.39\text{--}0.51 \text{ g/cm}^3$ ) which expands their applications in the environment and stress monitoring, motion detection, etc. Table 2 presents the weight and density of these samples.



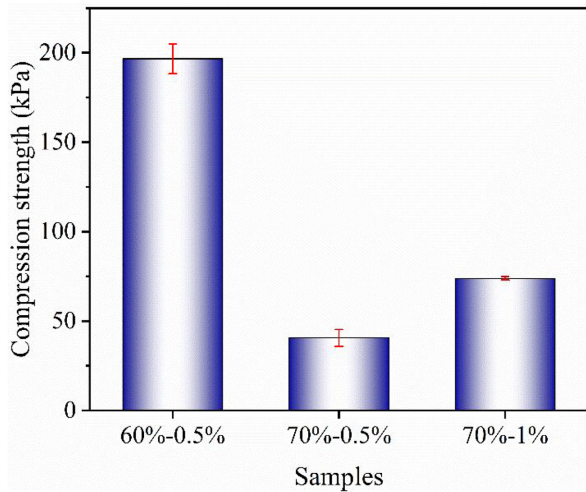


**Figure 8.** Mechanical strength of three different PDMS/MWCNT foam nanocomposites.

PDMS/MWCNT foam nanocomposites could sustain higher loadings (2 kN) without any visible fracture or tearing during experiment cycles. This can be interpreted as higher mechanical strength of PDMS/MWCNT foam nanocomposites comparing to the other types of foam nanocomposites in the literature (Cai et al., 2020; Kim and Kim, 2017; Tang et al., 2019). Figure 8 displays the compressive strength (the stress at 50% strain during the compression test) of PDMS/MWCNT foam nanocomposites (Huang et al., 2017; Yao et al., 2013).

Figure 9 describes the relative resistance change of three types of PDMS/MWCNT foam nanocomposite at six test cycles. The cycles were consecutively performed at a 1 mm/min displacement rate with a 1 min relaxation time between each individual cycle.

The graphs in Figure 9 show that during the compression test, the electrical resistance decreased as the strain increased. The applied force caused breakdown or reformation of percolation networks and it changed

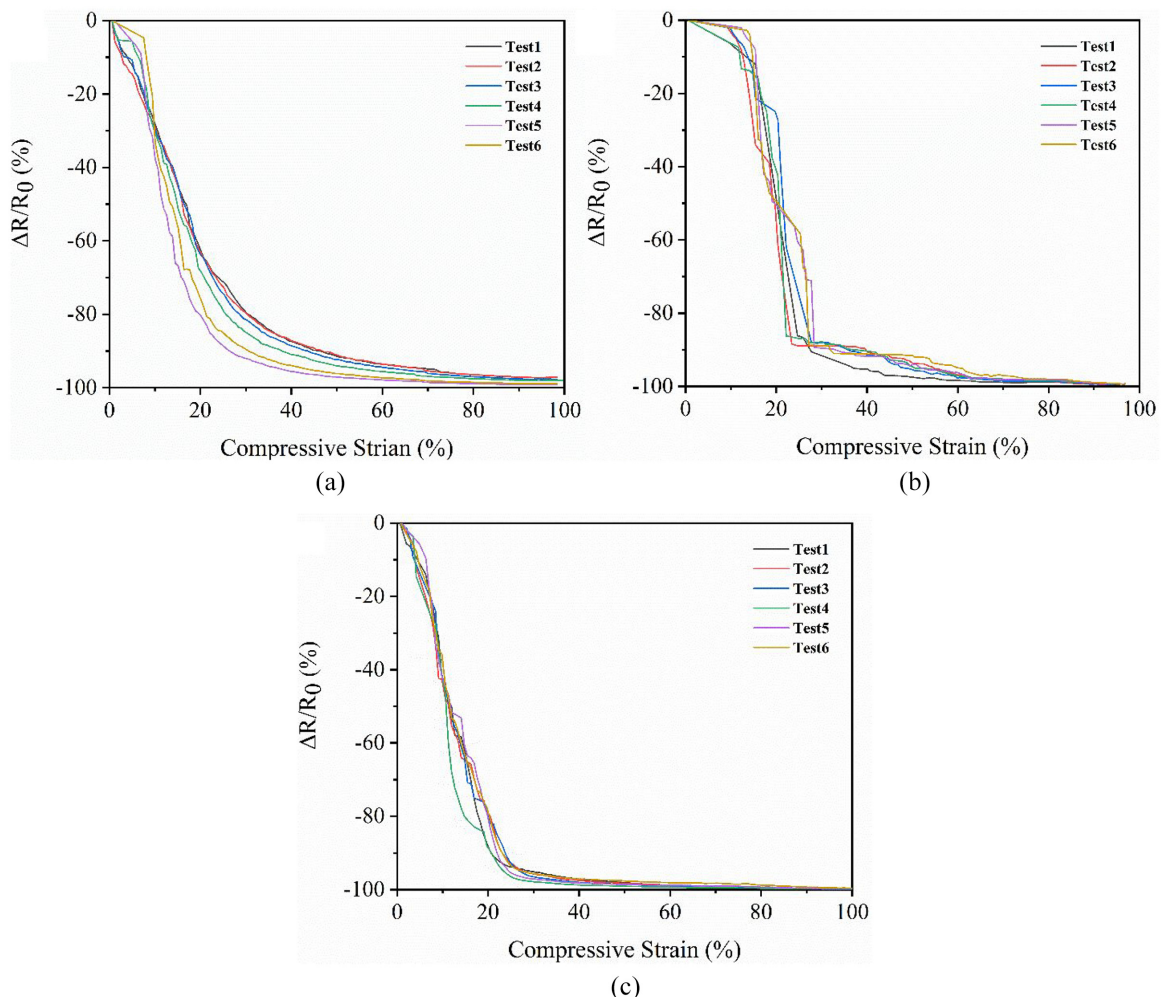


**Figure 9.** Relative resistance changes versus strain in six different cycles for: (a) 70%–0.5%, (b) 70%–1%, and (c) 60%–0.5%.



the interparticle distances which resulted in the Piezoresistive behavior.

Since polymer matrix and the fillers have very different Young's modulus, their compressibility is different; therefore, an increase in strain decreased interparticle gaps between MWCNTs, and additional conductive networks probably formed which caused a drop in the electrical resistance of the porous nanocomposite. Moreover, the pressure was applied to the foam structure and the cell struts suffered from surrounding pressure. Consequently, the conductive particles between the cells were pressurized, and more direct contact points between the conductive fillers might be formed. By applying pressure, the fillers would get closer to each other and decrease the average electron tunneling distance which could improve the foam conductivity (Zhai et al., 2015). Furthermore, each type of sensor at its different cycles maintained favorable repeatability with limited variations in respect to each other (Figure 9). It is worth mentioning that the electrical hysteresis effect prevented obtaining completely the same results in different cycles. Hysteresis in the foam nanocomposites can be related to the polymer-fiber bonding and its changes during the cycles. However, comparing to similar reports in the literature, we succeeded to limit the hysteresis effect up to 10% when the compressive stress is more than 30% (Huang et al., 2017). Low hysteresis in relative resistance changes indicates that after compression test cycles (unloading) there were limited changes in the morphology of the MWCNTs conductive networks inside the nanocomposite structure. It can be concluded that polymer matrix flexibility and foam structure provided higher controllability over the conductive networks.

Figure 10 shows GF versus strain for three different types of PDMS/MWCNT foam nanocomposites. Each

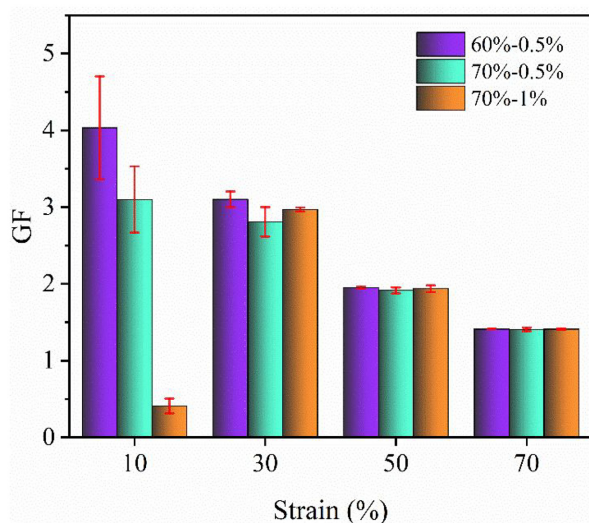


**Figure 10.** GF versus strain for three different PDMS/MWCNT foam nanocomposites.

sensor was tested for six runs at the same conditions to compare the consistency of their outputs. Figure 10 indicates that at low strains (10%) nanocomposites with 0.5 wt.% MWCNT have much higher GF than the samples with 1 wt.% MWCNT. Significant changes in the conductive paths of the nanocomposite (during the loading process) would increase GF which means there is higher sensitivity and variation in the electrical conductivity of the system (near the percolation threshold). If the filler content of the nanocomposite is far from the percolation threshold, the conducting network configuration would be stronger. As a result, the compression-induced electrical responses of nanocomposite will be smaller and adversely affect its sensing applications (Zhai et al., 2015). It can be concluded that, 0.5 wt.% MWCNT was closer to the percolation threshold of PDMS/MWCNT nanocomposite and the applied pressure at lower strains had limited effects on the samples with 1 wt.% MWCNT content. At larger strains, the GF in all cases decreased when the strain increased due to the formation of relatively stable conductive networks and almost all three types of foam nanocomposites had equal relative resistance change. At high strain levels (more than 70%), the cell walls in the foam structure were completely connected and created stable conductive paths; therefore, applying extra pressure did not change the electrical resistance of the sensor. Furthermore, Figure 10 illustrates that foam nanocomposite samples with 60 wt.% porosity and 0.5 wt.% MWCNT had a slightly higher GF than samples with 70% porosity and 0.5 wt.% MWCNT.

Although foaming helps to decrease the percolation threshold and improves sensitivity, this observation showed that there is an optimum value for the required sample porosity (Zheng et al., 2004). The foaming effect will adversely change the sample sensitivity at the same MWCNT content when porosity is far from the optimum point. The results from Figure 10 indicate that PDMS/MWCNT foam nanocomposites have a larger range of sensitivity compared to similar studies and the change in GF is noticeable from 10% to 70% strains (Cai et al., 2020; Chen et al., 2018; Patole et al., 2019).

#### 4. Conclusion

In this paper, a fabrication process of PDMS/MWCNT foam nanocomposite is reported which led to sufficient MWCNT dispersion in the polymer matrix with uniform foam morphology. The fabricated samples had excellent mechanical properties which could sustain up to 2 kN force without experiencing any noticeable macroscopic damages (fracture or tearing). Highly flexible and lightweight PDMS/MWCNT foam nanocomposites had low density of 0.36–0.53 g/cm<sup>3</sup> with enhanced compressibility up to 85% in addition to recoverability. Uniform foam morphology, strong cell

walls, homogenous MWCNT dispersion, and polymer reinforcement bonding caused a profound improvement in declining electrical and mechanical hysteresis. In this article, foam nanocomposites with 0.5 wt.% MWCNT content and 60% porosity obtained better piezoresistive responses (higher pressure sensitivity, higher GF, and lower electrical hysteresis) along with higher mechanical properties. At 1 wt.% MWCNT content, percolation threshold was passed, and resistance change in response to applied pressure decreased. Moreover, at the same MWCNT content, 60% foam porosity led to a higher desirable GF ( $4 \pm 0.7$ ) at low stresses comparing to 70% foam porosity.


### Declaration of conflicting interests

The authors declared no potential conflicts of interest with respect to the research, authorship, and/or publication of this article.

### Funding

The authors disclosed receipt of the following financial support for the research, authorship, and/or publication of this article: The work described in this paper was supported by Natural Sciences and Engineering Research Council of Canada (NSERC under grant RGPIN-217525). The authors are grateful for their supports.

### ORCID iD

Hani E. Naguib  <https://orcid.org/0000-0003-4822-9990>

### References

- Ameli A, Nofar M, Park CB, et al. (2014) Polypropylene/carbon nanotube nano/microcellular structures with high dielectric permittivity, low dielectric loss, and low percolation threshold. *Carbon* 71: 206–217.
- Amjadi M, Kyung KU, Park I, et al. (2016) Stretchable, skin-mountable, and wearable strain sensors and their potential applications: A review. *Advanced Functional Materials* 26(11): 1678–1698.
- Bao WS, Meguid SA, Zhu ZH, et al. (2012) Tunneling resistance and its effect on the electrical conductivity of carbon nanotube nanocomposites. *Journal of Applied Physics* 111: 093726.
- Bar-Ziv Y, Beer Y, Ran Y, et al. (2010) A treatment applying a biomechanical device to the feet of patients with knee osteoarthritis results in reduced pain and improved function: A prospective controlled study. *BMC Musculoskeletal Disorders* 11(179): 179.
- Bauhofer W and Kovacs JZ (2009) A review and analysis of electrical percolation in carbon nanotube polymer composites. *Composites Science and Technology* 69(10): 1486–1498.
- Bloor D, Donnelly K, Hands PJ, et al. (2005) A metal–polymer composite with unusual properties. *Journal of Physics D: Applied Physics* 38(16): 2851–2860.
- Boland CS, Khan U, Binions M, et al. (2018) Graphene-coated polymer foams as tuneable impact sensors. *Nanoscale* 10(11): 5366–5375.
- Cai JH, Li J, Chen XD, et al. (2020) Multifunctional polydimethylsiloxane foam with multi-walled carbon nanotube and thermo-expandable microsphere for temperature sensing, microwave shielding and piezoresistive sensor. *Chemical Engineering Journal* 393: 124805.
- Cao CF, Zhang GD, Zhao L, et al. (2019) Design of mechanically stable, electrically conductive and highly hydrophobic three-dimensional graphene nanoribbon composites by modulating the interconnected network on polymer foam skeleton. *Composites Science and Technology* 171: 162–170.
- Chen Q, Cao P and Advincula RC (2018) Mechanically robust, ultraelastic hierarchical foam with tunable properties via 3D printing. *Advanced Functional Materials* 28(21): 1–9.
- Choi S, Han SI, Kim D, et al. (2019) High-performance stretchable conductive nanocomposites: Materials, processes, and device applications. *Chemical Society Reviews* 48(6): 1566–1595.
- Chortos A, Liu J and Bao Z (2016) Pursuing prosthetic electronic skin. *Nature Materials* 15(9): 937–950.
- Ding S, Han B, Dong X, et al. (2017) Pressure-sensitive behaviors, mechanisms and model of field assisted quantum tunneling composites. *Polymer* 113: 105–118.
- D’Lima DD, Fregly BJ, Patil S, et al. (2012) Knee joint forces: Prediction, measurement, and significance. *Proceedings of the Institution of Mechanical Engineers, Part H: Journal of Engineering in Medicine* 226(2): 95–102.
- Ghahramani P, Eldyasti A and Leung SN (2021) Open-cell polyvinylidene fluoride foams as carriers to promote bio-film growth for biological wastewater treatment. *Polymer Engineering and Science* 61(8): 2161–2171.
- Hammock ML, Chortos A, Tee BC, et al. (2013) 25th anniversary article: The evolution of electronic skin (E-skin): A brief history, design considerations, and recent progress. *Advanced Materials* 25(42): 5997–6038.
- Huang W, Dai K, Zhai Y, et al. (2017) Flexible and lightweight pressure sensor based on carbon nanotube/thermoplastic polyurethane-aligned conductive foam with superior compressibility and stability. *ACS Applied Materials & Interfaces* 9(48): 42266–42277.
- Iglio R, Mariani S, Robbiano V, et al. (2018) Flexible Polydimethylsiloxane foams decorated with multiwalled carbon nanotubes enable unprecedented detection of ultralow strain and pressure coupled with a large working range. *ACS Applied Materials & Interfaces* 10(16): 13877–13885.
- Kanoun O, Bouhamed A, Ramalingame R, et al. (2021) Review on conductive polymer/CNTs nanocomposites based flexible and stretchable strain and pressure sensors. *Sensors* 21(2): 341.
- Kim JO, Kwon SY, Kim Y, et al. (2019) Highly ordered 3D microstructure-based electronic skin capable of differentiating pressure, temperature, and proximity. *ACS Applied Materials & Interfaces* 11(1): 1503–1511.
- Kim JS and Kim GW (2017) Hysteresis compensation of piezoresistive carbon nanotube/polydimethylsiloxane composite-based force sensors. *Sensors* 17(2): 229.
- Li M, Li H, Zhong W, et al. (2014) Stretchable conductive polypyrrole/polyurethane (PPy/PU) strain sensor with net-like microcracks for human breath detection. *ACS Applied Materials & Interfaces* 6(2): 1313–1319.
- Li Q, Li J, Tran D, et al. (2017) Engineering of carbon nanotube/polydimethylsiloxane nanocomposites with enhanced

- sensitivity for wearable motion sensors. *Journal of Materials Chemistry C* 5(42): 11092–11099.
- Liu H, Dong M, Huang W, et al. (2017) Lightweight conductive graphene/thermoplastic polyurethane foams with ultrahigh compressibility for piezoresistive sensing. *Journal of Materials Chemistry C* 5(1): 73–83.
- Liu H, Li Y, Dai K, et al. (2016) Electrically conductive thermoplastic elastomer nanocomposites at ultralow graphene loading levels for strain sensor applications. *Journal of Materials Chemistry C* 4(1): 157–166.
- Madaleno L, Pyrz R, Crosky A, et al. (2013) Processing and characterization of polyurethane nanocomposite foam reinforced with montmorillonite–carbon nanotube hybrids. *Composites Part A: Applied Science and Manufacturing* 44: 1–7.
- Ma Z, Wei A, Li Y, et al. (2021) Lightweight, flexible and highly sensitive segregated microcellular nanocomposite piezoresistive sensors for human motion detection. *Composites Science and Technology* 203: 108571.
- Oskouyi AB, Sundararaj U and Mertiny P (2014) Tunneling conductivity and piezoresistivity of composites containing randomly dispersed conductive nano-platelets. *Materials* 7(4): 2501–2521.
- Park J, You I, Shin S, et al. (2015) Material approaches to stretchable strain sensors. *ChemPhysChem* 16(6): 1155–1163.
- Patole SP, Reddy SK, Schiffer A, et al. (2019) Piezoresistive and mechanical characteristics of graphene foam nanocomposites. *ACS Applied Nano Materials* 2(3): 1402–1411.
- Ramalingame R, Hu Z, Gerlach C, et al. (2017) Shoe insole with MWCNT-PDMS-composite sensors for pressure monitoring. In: *Proceedings of IEEE sensors*, Glasgow, UK. 29 October–1 November 2017, pp.1–3. New York: IEEE.
- Rinaldi A, Tamburrano A, Fortunato M, et al. (2016) A flexible and highly sensitive pressure sensor based on a PDMS foam coated with graphene nanoplatelets. *Sensors* 16(12): 2148.
- Schurman DJ and Smith RL (2004) Osteoarthritis: Current treatment and future prospects for surgical, medical, and biologic intervention. *Clinical Orthopaedics and Related Research* S183–S189.
- Tanabe F, Yoshimoto S, Noda Y, et al. (2017) Flexible sensor sheet for real-time pressure monitoring in artificial knee joint during total knee arthroplasty. In: *2017 39th annual international conference of the IEEE engineering in medicine and biology society (EMBC)*, Jeju, Korea (South), 11–15 July 2017, pp.1591–1594. New York: IEEE.
- Tang Y, Guo Q, Chen Z, et al. (2019) In-situ reduction of graphene oxide-wrapped porous polyurethane scaffolds: Synergistic enhancement of mechanical properties and piezoresistivity. *Composites Part A: Applied Science and Manufacturing* 116: 106–113.
- Tung TT, Robert C, Castro M, et al. (2016) Enhancing the sensitivity of graphene/polyurethane nanocomposite flexible piezo-resistive pressure sensors with magnetite nanospacers. *Carbon* 108: 450–460.
- Xu F, Li X, Shi Y, et al. (2018) Recent developments for flexible pressure sensors: A review. *Micromachines* 9(11): 580.
- Yamada T, Hayamizu Y, Yamamoto Y, et al. (2011) A stretchable carbon nanotube strain sensor for human-motion detection. *Nature Nanotechnology* 6(5): 296–301.
- Yao HB, Ge J, Wang CF, et al. (2013) A flexible and highly pressure-sensitive graphene-polyurethane sponge based on fractured microstructure design. *Advanced Materials* 25(46): 6692–6698.
- Zare Y and Rhee KY (2021) Formulation of tunneling resistance between neighboring carbon nanotubes in polymer nanocomposites. *Engineering Science and Technology an International Journal* 24(3): 605–610.
- Zhai T, Li D, Fei G, et al. (2015) Piezoresistive and compression resistance relaxation behavior of water blown carbon nanotube/polyurethane composite foam. *Composites Part A: Applied Science and Manufacturing* 72: 108–114.
- Zhao H, Zhang Y, Bradford PD, et al. (2010) Carbon nanotube yarn strain sensors. *Nanotechnology* 21(30): 305502.
- Zheng Q, Zhou JF and Song YH (2004) Time-dependent uniaxial piezoresistive behavior of high-density polyethylene/short carbon fiber conductive composites. *Journal of Materials Research* 19(9): 2625–2634.
- Zhou Z, Zhang X, Wu X, et al. (2016) Self-stabilized polyaniline@graphene aqueous colloids for the construction of assembled conductive network in rubber matrix and its chemical sensing application. *Composites Science and Technology* 125: 1–8.
- Zuruzi AS, Haffiz TM, Affidah D, et al. (2017) Towards wearable pressure sensors using multiwall carbon nanotube/polydimethylsiloxane nanocomposite foams. *Materials & Design* 132: 449–458.
- Ødegaard H, Gisvold B and Strickland J (2000) The influence of carrier size and shape in the moving bed biofilm process. *Water Science & Technology* 41(4–5): 383–391.